THE CRUSTAL STRUCTURE IN NORTHWEST CHINA

Walter D. Mooney (1) and Robert G. Coleman (2)

(1) U.S. Geological Survey; Menlo Park, CA USA
(2) Department of Geology and Environmental Sciences Stanford University; Stanford, CA USA

Sponsored by U.S. Department of Energy
Office of Nonproliferation and National Security
Office of Research and Development
DOE IA No.: DE-AI04-98AL79758

ABSTRACT

We have reinterpreted seismic refraction data taken along a geoscience transect recorded in China. The data consists of 3-component seismic data along an 1100 km-long refraction profile in northwest China. The profile crosses the southern margin of the Altay Mountains, the Junggar Basin, the Tianshan Mountains, and the Tarim Basin. P- and S-wave seismic data acquired along this profile were used to model the crustal velocity structure and Poisson's ratio. The average crustal thickness is 50 km, ten kilometers thicker than the global average for continental crust. The largest difference in crustal thickness is located at the northern end of the profile, where, over a distance of <400 km, it varies from 54 km thick under the Altay mountains to 46 km thick under the Junggar basin. On the southern side of the basin, the crustal thickness increases to about 49 km, and it remains this thickness over the rest of the southern portion of the profile, with only slight variation. Poisson's ratios of 0.25-0.28, observed below the Junggar basin, imply either a mafic crystalline Precambrian basement or imbricated Paleozoic accretionary belt, whereas the lower Poisson's ratios of 0.25-0.26, modeled through the crust in the Tianshan Province, imply a granitic composition. Observed Pn velocities vary with tectonic province and include velocities of 7.9 km/s below the Altay Mountains; 7.7 below the thinner crust of the Junggar Basin; 7.8 below the Tianshan Mountains; and 8.0 below the Tarim Basin.

Key Words: crustal structure, China, seismic reflection, seismic refraction

OBJECTIVE

High quality regional models of crustal structure are necessary for accurate seismic locations required by the monitoring of the Comprehensive Nuclear-Test-Ban Treaty (CTBT). This paper presents the first detailed model of P- and S-wave velocity structure of the crust in northwest China created from controlled source data.

RESEARCH ACCOMPLISHED

In 1988, an 1100 km-long, 3-component seismic refraction profile was collected across northwest China (Fig. 1). Seismic energy was provided by twelve shots fired in boreholes. The charge sizes ranged from 1500 to 4000 kg, sufficient to provide clear first arrivals to a maximum offset of 300 km. The shotpoint interval ranged from 63 to 125 km, and the receiver interval was between 2 and 4 km. The profile was recorded along existing roads, which provided three nearly straight profile segments.

In order to aid in the correlation of phases, reduction velocities of 6.0 km/s and 3.46 km/s were used for P- and S-waves, respectively. The time scale used for S-wave record sections was compressed by a factor of 0.58 in order to match the P-wave arrival times. In order to avoid the small time shift that is introduced by digital filters, unfiltered P-wave data were used for phase correlation and traveltime picking. In order to improve the signal-to-noise ratio for phase correlation, the S-wave data were filtered with a 0-6 Hz bandpass.

The first arrivals of the Pg phase were used to invert for the upper crustal velocity structure using a finite-difference tomographic method (Hole, 1992). The reflection phases P_1P, P_LP, P_2P and P_mP were used to determine the approximate velocity structure of the middle to lower crust with the X^2-T^2 method (Giese, Prodehl and Stein, 1976). After establishing an initial crustal P-wave velocity structure, the final P-wave model was determined using 2-D forward raytracing modeling (Cerveny, Molotkov, and Psencik, 1977; Cerveny and Psencik, 1984), amplitude modeling using the reflectivity method (Fuchs and Muller, 1971), and 2-D ray methods. By adjusting the velocities and depths of the boundaries with the raytracing method, the traveltimes of the various phases on the record sections were fit, thus establishing the final P-wave velocity model.

The S-wave velocity structure differs from P-wave velocity structure only in its velocity distribution; the depths of all layer boundaries were kept the same. The upper crust shares similar characteristics to the P-wave structure, and just replacing P-wave velocity with S-wave velocity (assuming Poisson's ratio is 0.25) satisfies these data. Two-dimensional forward modeling was used to fit the remaining S-wave phases. Finally, from the respective P- and S-wave velocity models, the distribution of Poisson's ratio can be calculated.

The accuracy and resolution of the final model is dependent on a large number of factors, including shotpoint interval, receiver density, and lateral variations in near-surface low-velocities. An important factor is the correct identification of the various phases, and the number of ray paths intersecting a particular volume of the model. Perturbation of the velocity model shows that resolution of velocities and interface depths are about 2% and 5%, respectively, depending on the complexity of the model structure and the ray-path coverage.

CONCLUSIONS AND RECOMMENDATIONS

Crustal structure

The depth of sedimentary basins can be determined from these data based on the low seismic velocities of the basin fill. The Junggar, Turpan-Hami, and Tarim basins each have 5-8 km of sedimentary fill despite the overall convergent tectonic setting. The Tianshan, which show evidence for active uplift (Windley et al., 1990), are situated between the Tarim and Turpan-Hami basins. This implies that compressional stresses evident within the Tianshan are applied by the stronger crystalline crust beneath the neighbouring basins. The crystalline crust along this profile consists of three primary layers, with seismic velocities of 6.0-6.3 km/s, 6.3-6.6 km/s, and 6.9-7.0 km/s. The most important features within these layers are: (1) the

Bogdashan arc shows the highest velocities (6.3 km/s) within the upper layer, indicative of higher densities within the upper crust; (2) the seismic velocity within the middle crustal layer is 6.5-6.6 km/s from the Altai Mountains south to the Turpan-Hami basin, but decreases to 6.3 km/s from the Tianshan to the Quidam basin, and a mid-crustal low velocity layer (5.9 km/s) also is present. (3) The thickness of the lower crustal layer reaches a maximum (30 km) beneath the Junggar Accretional belt and the Altai Mountains. A minimum thickness of the lower crust (15 km) is found beneath the Junggar basin.

Such a three-layer stratification of the crust is commonly reported, and the velocities measured here are typical of many continental crustal sections. However, the lower crustal layer (6.9-7.0 km/s) is remarkably thick, with an average of 20 km (40% of the total crustal thickness). The middle crust (6.3-6.6 km/s) has an average thickness of 17 km, and the upper (consolidated) crust has an average thickness of 9 km. (Sedimentary accumulations range from 0 - 8 km in thickness). The average thickness of the entire crust is 50 km; thus the middle and lower crust comprise 74% of the crust.

The seismic velocity of the uppermost mantle (Pn) is less than or equal to the global average (8.05 km/s) in all parts of the study area. The lowest values (7.7-7.8 km/s) occur beneath the Junggar and Turpan-Hami basins. The Pn velocity is 8.0 km/s beneath Altai mountains, Junggar accretional belt, Tianshan accretional belt and Tarim platform.

Crustal thickening

These observations may be compared with global averages for continental crust. The average thickness of continental crust is 39 km. Thus the crustal thickness of NW China is 11 km thicker that the continental average and has likely been thickened by crustal shortening associated with the Tibetan orogeny and/or magmatic additions to the crust. The amount of shortening needed to thicken 39 km thick crust to 50 km is 30%. However, the fact that the upper crust (6.0-6.3 km/s) has only half the thickness of the middle and lower crust suggests that isostatic uplift has led to the erosion of about 10 km of the (shortened) upper crust. If we tentatively accept that 10 km of crust has been removed, then the shortening along the profile amounts to 50%. A major uncertainty in this calculation is the initial crustal thickness.

Alternatively the crust may have been thickened by magmatic additions. If these intrusions were mainly intermediate to mafic in composition, they could have thickened the middle and lower crust, respectively. If the upper crust was also thickened with silicic intrusions, erosion has eliminated the evidence for this thickening. The present geophysical data do not allow us to discern which process, compression or magmatic inflation, has dominated the process of crustal thickening.

Crustal Composition

The interpretation of crustal composition from seismic velocity measurements has recently been reviewed by Holbrook et al. (1992), Rudnick and Fountain (1995), and Christensen and Mooney (1995). We begin our discussion with the measured Vp structure and then discuss the Vp/Vs ratio, or, equivalently, Poisson's ratio.

As mentioned above, the consolidated crust is stratified into three primary layers with seismic velocities of 6.0-6.3 km/s, 6.3-6.6 km/s, and 6.9-7.0 km/s. The average velocity of the consolidated crust is 6.6 km/s, which is significantly higher than the global average of 6.45 km/s (with a standard deviation of 0.21 km/s). This high average velocity is mainly the result of the great thickness (20 km) of the high-velocity lower crustal layer.

Christensen and Mooney (1995) present statistical averages for continental crustal velocities as a function of depth. Upper crustal velocities in the study area are consistent with geological observed meta-sedimentary and felsic intrusive rocks. Measured Poisson's ratios for these rocks (0.25) are consistent with this interpretation. Middle crustal velocities are lower beneath the Tianshan and eastern Tarim basin (6.3 km/s) than those terrains to the north (6.5-6.6 km/s), and Poisson's ratio increases slightly from south (0.25) to north (0.26-0.27). These observations indicate that the bulk composition of middle crust beneath the Tianshan is close to that of a tonalite or granodiorite, and becomes less silicic to the north (equivalent to a diorite). For example, an increase in the abundance of amphibolite in the middle crust from 5% beneath the Tianshan to about 35% beneath the terrains to the north would satisfy the observations (c.f., Figure 18 in

Christensen and Mooney, 1995). The lower crustal seismic velocity (6.9-7.0 km/s) and Poisson's ratio (0.26-0.28) are remarkably uniform along the entire 1,100 km transect. The seismic velocity of the lower crust is consistent with a mafic composition (mafic granulite and mafic garnet granulite), or anorthosite. However, these compositions would provide a Poisson's ratio of 0.29-0.31, which is 0.01-0.05 higher than the reported values. Granulite grade metapelite provides the best fit to the seismic velocity data, but it seems unlikely, based on heat flow constraints, that the lower continental crust is composed of a thick (20 km) layer of metapelite over a distance of 1,100 km. Thus we favor mafic granulite composition.

REFERENCES

Cerveny, V. , I.A. Molotkov, and 1. Psencik. 1977. Ray method in seismology. Prague.: Univerzita Karlova.

Cerveny, V., and I. Psencik, eds. 1984. SEIS83-numerical modeling of seismic wavefield in 2-D laterally varying layered structures by the ray method, in: E. R. Engdahl (editor), Documentation of earthquake algorithms. World data center (A) for solid earth geophysics, Boulder, Colo., Rep. SE-35, 36-40. Edited by E. R. Engdahl. Vol. Rep. SE-35, Documentation of earthquake algorithms. World data center (A) for solid earth geophysics, Boulder, Colo., Rep. SE-35, 36-40. Boulder, Colo.: World Data Center.

Christensen, N. I. and W. D. Mooney, Seismic velocity structure and composition of the continental crust: A global view, J. Geophys. Res., 100,9761-9788, 1995.

Fuchs, K., and G. Muller. 1971. Computation of synthetic seismograms with the reflectivity method and comparison with observations, Geophys. J. R. Astr. Soc. 23:417-433.

Giese, P., C. Prodehl, and A. Stein. 1976. Explosion Seismology in Central Europe. Berlin Heidelberg, New York.: Springer-Verlag.

Holbrook, W.S., W.D. Mooney, and N.I. Christensen. 1992. The Seismic velocity structure of the deep continental crust. In Continental Lower Crust, Elsevier. Developments in Geotectonics, edited by D. M. Fountain, R. Arculus and R. W. Kay: Elsevier.

Hole, J. A., 1992. Nonlinear high-resolution three-dimensional seismic travel time tomography. Journal of Geophysical Research, B, 97 (B5):6553-6562.

Rudnick, R.L., and D.M. Fountain. 1995. Nature and composition of the continental crust: a lower crustal perspective. Reviews of Geopyhsics 33 (3):267-309.

Windley, B.F., M.B. Allen, C. Zhang, Z-Y. Zhao, , and G-R. Wang. 1990. Paleozoic accretion and Cenozoic redeformation of the Chineses Tien Shan Range, central Asia. Geology 18:128-13 1.

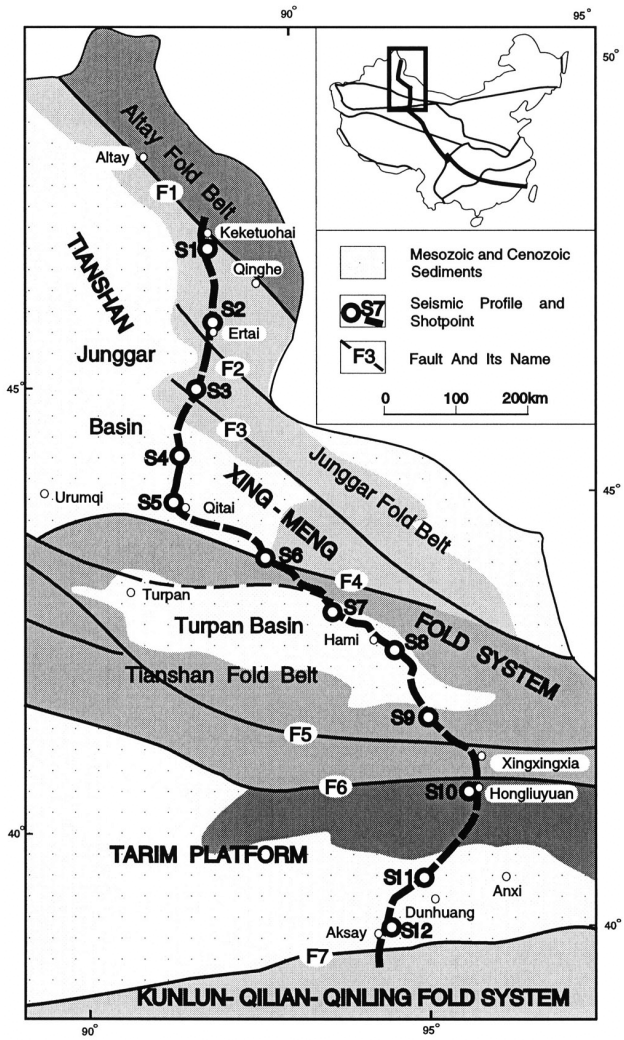

Figure 1. Tectonic setting of China indicating location of Geoscience transect line.

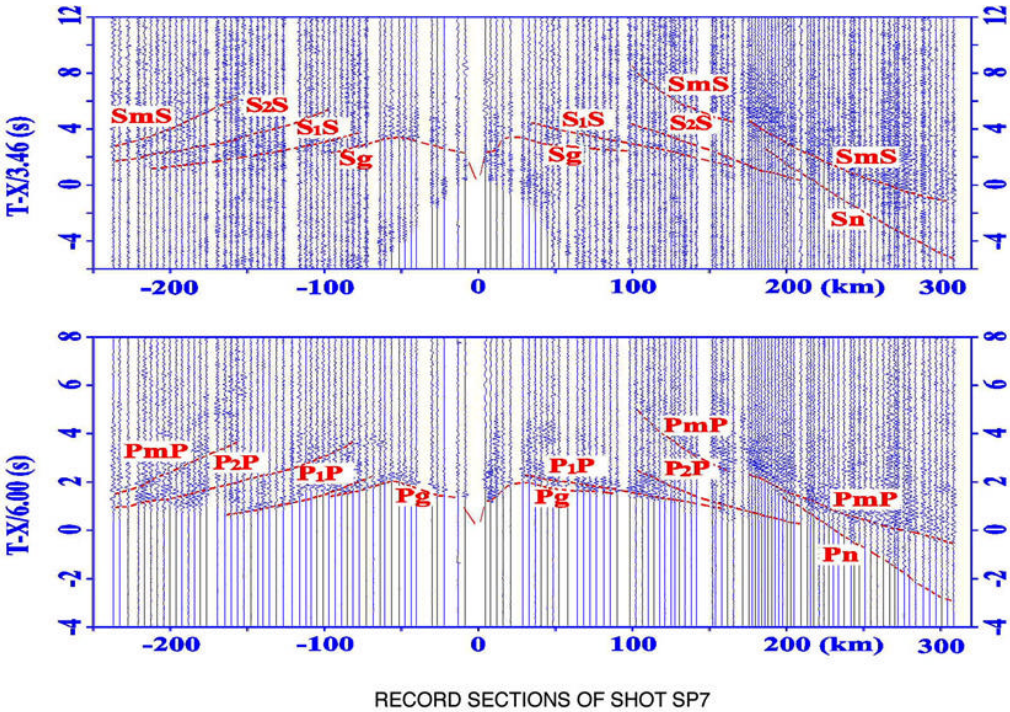

Figure 2. Record sections of shotpoint SP7. (upper: trace-normalized band-pass filtered (0-8 Hz) S-wave record section with a reduction velocity of 3.46 km/s and a factor of 0.58 in time scale with respect to P-wave record section; lower: trace-normalized P-wave record section with a reduction velocity of 6.00 km/s.)

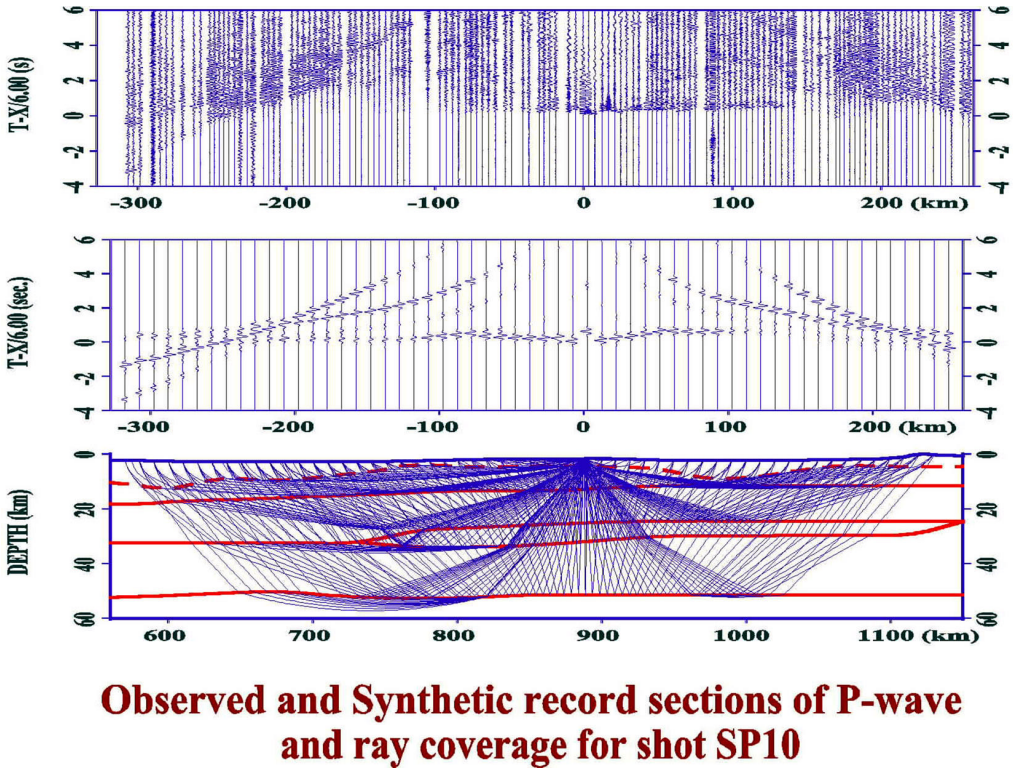

Figure 3. Raypath and sythetic seismogram for shotpoint SPIO

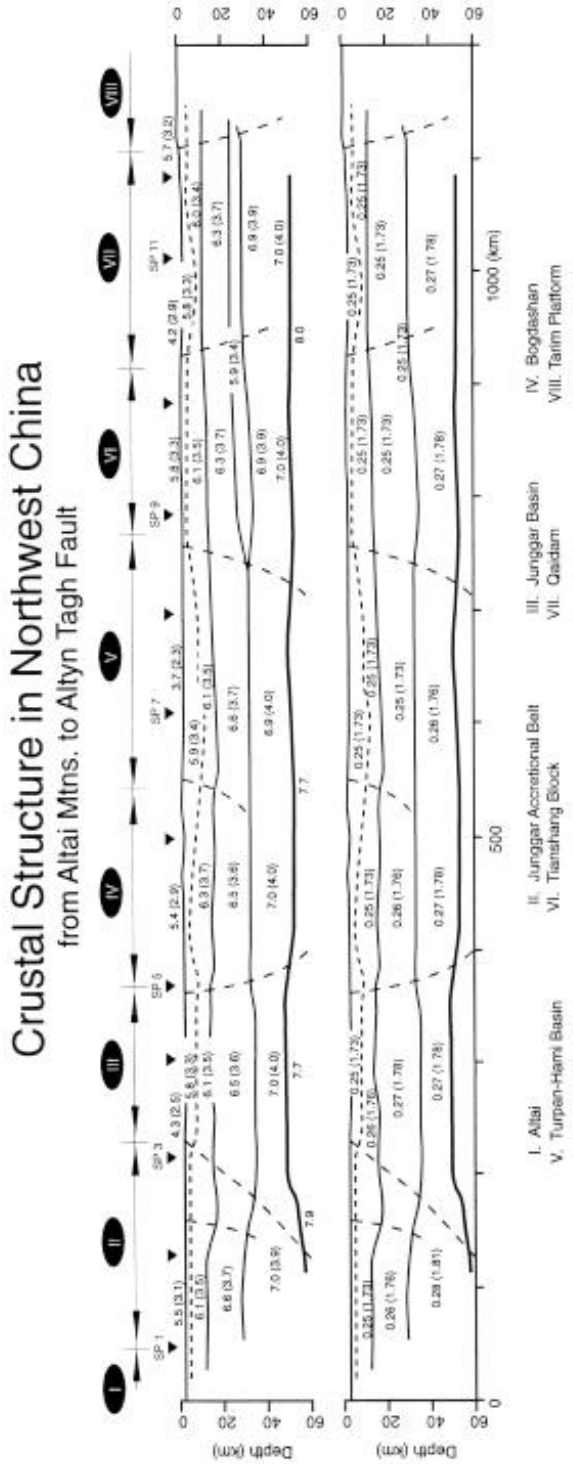

Figure 4. The crustal structure of the profile along the GTTA. (upper: P-wave velocity structure; lower: S-wave velocity structure and Poisson's ratio, where the dashed line indicate the top of basement.)